# Site-Specific Gene Modification by PNAs Conjugated to Psoralen

Ki-Hyun Kim,[‡] Peter E. Nielsen,[§] and Peter M. Glazer*,[‡]

*Departments of Therapeutic Radiology and Genetics, Yale University School of Medicine, Post Office Box 208040, New Haven, Connecticut 06520-8040, and Department of Medical Biochemistry and Genetics, University of Copenhagen, The Panum Institute, Blegdamsvej 3, Copenhagen DK-2200, Denmark*

*Received July 15, 2005; Revised Manuscript Received October 5, 2005*

ABSTRACT: DNA-binding molecules, including triplex-forming oligonucleotides (TFOs) and peptide nucleic acids (PNAs), can be utilized to introduce site-specific mutations or to promote recombination at selected genomic sites. To further evaluate the utility of PNAs for site-specific gene modification, we tested dimeric bis-PNAs conjugated to psoralen. These PNAs are designed to form a triplex-invasion complex within the *supF* reporter gene in an episomal shuttle vector and to direct site-specific photoadduct formation by the conjugated psoralen. The psoralen−bis-PNA conjugate was found to direct photoadduct formation to the intended 5′-TpA base step next to the PNA-binding site, and the photoadduct formation efficiency displayed both concentration and UVA irradiation dependence. The effect of PNA-targeted photoadducts in a mammalian system was tested by SV40-based shuttle vector assay. After *in vitro* binding, we found that photoadducts directed by PNAs conjugated to psoralen-induced mutations at frequencies in the range of 0.46%, 6.5-fold above the background. In a protocol for intracellular gene targeting in the episomal shuttle vector, the psoralen−PNA-induced mutation frequency was 0.13%, 3.5-fold higher than the background. Most of the induced mutations were deletions and single-base-pair substitutions at or adjacent to the targeted PNA-binding and photoadduct-formation sites. When the results are taken together, they demonstrate the ability of bis-PNAs conjugated with psoralen to mediate site-specific gene modification, and they further support the development of PNAs as tools for gene-targeting applications.

The design of DNA-binding ligands is based on the principle that they are able to recognize and bind to specific sites in double-stranded DNA. A number of DNA-binding molecules for targeting specific genes have been developed, including polyamides as DNA minor-groove binders (*3*) and zinc-finger peptides (*4*), triplex-forming oligonucleotides (TFOs),[1] and peptide nucleic acids (PNAs) as DNA major-groove binders (*1*, *2*).

PNAs are DNA mimics that substitute 2-aminoethylglycine linkages for the phosphodiester backbones of oligonucleotides (*5*). This backbone substitution gives PNAs favorable nucleic acid hybridization properties and makes PNAs one of the most interesting tools for gene targeting. PNAs can form PNA−DNA or PNA−RNA duplexes via Watson−Crick base pairing, and these duplexes are more stable than duplexes formed with the corresponding oligonucleotides (*6*−*8*). Although PNAs were originally conceived as triplex-forming, major-groove-binding ligands, the preferred binding of homopyrimidine PNAs to complementary homopurine targets on double-stranded DNA is via the formation of PNA/DNA/PNA triplex-invasion complexes (*9*, *10*). A triplex-invasion complex is composed of a $PNA_2$−DNA triplex formed on one strand of the target duplex and a displaced single-stranded DNA loop (*11*). Although other PNA-binding modes have been demonstrated, the triplex-invasion complex is the favored structure when duplex DNA is targeted by PNAs. Because the triplex-strand-invasion process requires opening of the duplex, factors that stabilize duplex DNA, such as the cations, $Na^+$, $Mg^{2+}$, and spermine/spermidine, can inhibit PNA binding (*12*, *13*). Binding rates can, however, be enhanced by using bis-PNAs, in which two PNA strands (one strand for Watson−Crick base pairing and the other strand for Hoogsteen base pairing) are chemically linked, and by tailing bis-PNAs with three to four positively charged lysines. Such cationic bis-PNAs have been shown to bind to their targets in double-stranded DNA under physiological conditions (*14*−*16*). Additionally, the substitution of cytosine with the pseudoisocytosine J monomer (a nucleobase analogue of N3-protonated cytosine) in the Hoogsteen strand can improve PNA binding at neutral pH because it obviates the need for cytosine protonation. Most importantly, these modifications for improved binding do not compromise the sequence specificity of PNAs (*16*).

PNAs can be used to bind site specifically to DNA to alter gene expression via transcriptional regulation (*13*, *17*−*23*), replication inhibition (*24*), mutation (*25*, *26*), recombination (*27*), or DNA modification (*28*−*30*). The extremely stable PNA triplex-invasion complex is able to arrest the elongation of RNA polymerase (*13*, *17*, *18*) and, if targeted to a region within the transcription-factor-binding site, can block transcription initiation (*19*−*21*). Interestingly, the displaced loop of the triplex-invasion complex can be recognized by RNA polymerase as a transcription-initiation site (promoter) (*22*,

* To whom correspondence should be addressed. E-mail: peter.glazer@yale.edu. Telephone: (203) 737-2788. Fax: (203) 737-1467.

[‡] Yale University School of Medicine.

[§] University of Copenhagen.

[1] Abbreviations: PNA, peptide nucleic acid; TFO, triplex-forming oligonucleotide.

10.1021/bi051379a CCC: $33.50 
Published on Web 12/06/2005

*23*). As a result, PNAs can function as artificial transcription factors. Additionally, previous studies in our group have demonstrated that bis-PNAs targeted to chromosomal or episomal genes can induce site-specific mutations or stimulate recombination, respectively (*25*−*27*). In other work, it has also been reported that PNAs conjugated with DNA-modifying agents, such as benzophenone, anthraquinone, or psoralen, can be used for DNA modification *in vitro* (*28*−*30*).

In this study, we tested the ability of PNAs to introduce a site-specific psoralen photoadduct for the purpose of gene modification. Psoralen is a tricyclic, planar DNA intercalating compound, which binds covalently to DNA upon long-wavelength UV irradiation (UVA: 320−400 nm) (*31*). We designed PNAs conjugated with psoralen to recognize a binding site on the *supFLSG3* reporter gene by triplex-invasion-complex formation. Targeted photoadduct formation was assayed *in vitro*, and mutagenesis in the targeted gene was assayed using an episomal shuttle vector assay. The photoadducts were found to occur at a 5′-TpA base step next to the PNA-binding site, and the efficiency of photoadduct formation displayed the PNA concentration and UVA irradiation dependence. The shuttle vector assay revealed induction of mutations at frequencies in the range of 0.13−0.46%, depending upon whether the adducts were targeted within cells or were preformed on the shuttle vector *in vitro* prior to transfection, respectively. Sequence analysis showed that the mutations were located around the binding site of the psoralen-conjugated PNA. The results support the application of PNAs as tools for site-specific gene modification.

## EXPERIMENTAL PROCEDURES

*PNA Molecules.* The PNA molecule used in this study was PNA2462 Pso-$(eg1)_2$-$(Lys)_3$-TJT TTT TTJ-$(eg1)_3$-CTT TTT TCT-Lys (N terminus to C terminus). The PNAs were synthesized and purified as described previously (*29*, *30*). They were homogeneous based on HPLC and exhibited one major peak at the expected mass as analyzed by MALDI−TOF mass spectroscopy. 8-Methoxycarbonylpsoralen (denoted as Pso) was conjugated to the N terminus of the PNA on the solid support via eg1 (8-amino-2,6-dioxaoctanoic acid) flexible linker using the psoralen monomer, 8-(carboxymethoxy)psoralen (*30*, Kim and Nielsen, manuscript under revision). Three lysine amino acids were attached to increase the aqueous solubility and the binding affinity to the DNA. "J" indicates the synthetic nucleobase pseudoisocytosine.

*Plasmid Construct.* The SV40 shuttle vector, pLSG3T7, was derived from pSP189 and carries an A:T base-pair-rich homopurine/homopyrimidine target site suitable for bis-PNA binding within the modified *supFLSG3* just upstream of the coding region (bp 88−96) (*32*). Next to the PNA-binding site, there is a 5′-TpA base step (bp 99−100) within the coding region, which is a preferential intercalation site for psoralen. PNAs conjugated with psoralen were designed to introduce site-specific photoadducts at this position. Also, plasmid pLSG3T7 contains a T7 promoter further downstream of the coding region for use in *in vitro* transcription elongation arrest assays using T7 RNA polymerase.

*Triplex-Invasion-Complex Formation.* For formation of the triplex-invasion complex, various concentrations of PNAs (as indicated) were incubated with a fixed amount (0.5 $\mu$g) of pLSG3T7 in TE buffer (pH 7.4) with 10 mM KCl for 2 h at 37 °C. After triplex-invasion-complex formation, PNA/plasmid mixtures were assayed for binding efficiency and analyzed for photoadduct formation.

*Gel-Shift Assay for Binding Efficiency of PNAs.* To form triplex-invasion complexes, various concentrations of PNA were incubated with a desired amount of pLSG3T7 (as indicated) in TE buffer (pH 7.4) and 10 mM KCl at 37 °C for 2 h. PNA−pLSG3T7 mixtures were digested with restriction enzymes (*Xho*I and *Bam*HI) to generate a 158-bp fragment and analyzed by gel electrophoresis in 8% native polyacrylamide gels (19:1 acrylamide/bisacrylamide) using TBE buffer (90 mM Tris at pH 8.0, 90 mM boric acid, and 2 mM EDTA). DNA bands were visualized by silver staining. The binding efficiency was derived from the ratio between PNA-bound and nonbound DNA fragments. The relative quantification of the DNA fragments was calculated using ImageQuant software (Amersham Bioscience).

*Analysis of Photoadduct Formation by Transcription Elongation Arrest Assay Using T7 Phage RNA Polymerase.* For the triplex-invasion-complex formation, various concentrations of PNA2462 (0−0.8 $\mu$M) were incubated with pLSG3T7 (0.5 $\mu$g) in TE (pH 7.4) at 37 °C for 2 h. UVA irradiation (365 nm) was given to PNA−pLSG3T7 mixtures at a dose of 1.8 J/cm$^2$ on ice, and the PNA/plasmid mixtures were digested with *Xho*I. After purification of the linearized template, transcription elongation arrest assay was performed in 30 $\mu$L of transcription reaction mixture (1 mM NTP [except UTP], 0.2 mM UTP, 2 $\mu$Ci [$\alpha$-$^{32}$P]UTP, 5 mM DTT, and 10 units of T7 RNA polymerase) at 37 °C for 20 min. The reaction was terminated by adding a stop buffer, and the transcription reaction mixture was analyzed in a 10% denaturing polyacrylamide (20:1 acrylamide/bisacrylamide) gel containing 7 M urea in TBE buffer (90 mM Tris at pH 8.0, 90 mM boric acid, and 2 mM EDTA). As a size marker, an RNA-sequencing reaction ladder was used. In parallel, transcription products with nonirradiated PNA/plasmid mixtures were included as controls. Radioactive RNA bands were visualized by autoradiography using amplifying screens and Kodak X-OMAT AR film exposed at −70 °C for 16 h.

*Photoadduct Formation Efficiency Assay by Transcription Elongation Arrest Using T7 Phage RNA Polymerase.* Various concentrations of PNA (as indicated) and pLSG3T7 (0.5 $\mu$g) were incubated to form triplex-invasion complexes in TE (pH 7.4) at 37 °C for 2 h. UVA irradiation was performed, and the PNA/plasmid mixtures were digested with *Xho*I. The transcription elongation arrest assay was performed as described above, and the reaction mixture was analyzed in a 10% denaturing polyacrylamide (19:1 acrylamide/bisacrylamide) gel containing 7 M urea in TBE buffer. As a size marker, the transcription reaction was performed on *Bsp*EI-digested linear pLSGT7. Radioactive bands were visualized by autoradiography as above. The amount of transcription product was measured by densitometric scanning of the autoradiogram using ImageQuant software. Photoadduct formation efficiency was derived from the ratio between the run-off product and the truncated elongation band. The photoadduct formation efficiencies were analyzed by Prism (GraphPad Software, Inc.) and presented as a function of the PNA concentration.

*Irradiation Dose Dependence of Photoadduct Formation.* After triplex-invasion-complex formation with a fixed con-

centration of PNA, UVA irradiation was performed at doses from 0 to 3.6 J/cm$^2$ given over 0 to 12 min on ice. The photoadduct efficiency was assayed by transcription elongation arrest assay using T7 RNA polymerase, and the reaction products were analyzed in denaturing gel electrophoresis, as above. The photoadduct formation efficiency is presented as a function of the irradiation time.

*Mutagenesis Protocol and Shuttle Vector Analysis.* Monkey COS-7 cells were obtained from ATCC (1651-CRL) and were maintained in DMEM supplemented with 10% fetal bovine serum (Gibco BRL, division of Invitrogen). Varying concentrations of PNA (as indicated) and pLSG3T7 (3 $\mu$g) were incubated to form the triplex-invasion complexes at 37 °C for 2 h. After UVA irradiation at a dose of 1.8 J/cm$^2$ on ice, the UV-irradiated PNA−pLSG3T7 mixtures were transfected into monkey COS cells using cationic lipid formulation, Geneporter 2 (Gene Therapy Systems, Inc.) at 2 $\mu$g of plasmid/10$^6$ cells. The plasmid DNA was extracted after 48−72 h using a modified alkaline lysis procedure for DNA analysis, as described previously (*32*, *33*). The isolated DNA was digested with *Dpn*I and RNase A at 37 °C for 1 h, extracted with phenol/chloroform/isoamyl alcohol, and precipitated with ethanol. The *Dpn*I digestion eliminates unreplicated plasmid DNAs that have not acquired the mammalian methylation pattern (*33*). The purified DNA was transformed into indicator bacteria, *Escherichia coli* MBM7070, by electroporation (Bio-Rad, setting 25 $\mu$F/250 W/1800 V, using 0.1-cm cuvette), and mutant colonies containing inactivated *supFLSG3* genes, unable to suppress the amber mutation in the host cell $\beta$-galactosidase gene, were detected by visual inspection as white colonies among the wild-type blue ones (*32*). The mutation frequency was determined as the ratio of white (mutant) colonies in the total colonies. This frequency was presented with the PNA-binding and photoadduct-formation efficiencies as a function of the PNA concentration. The mutant plasmids were then extracted and further analyzed for mutation patterns by DNA sequencing (*32*). A parallel experiment was performed with nonirradiated PNA−pLSG3T7 and compared with the irradiated PNA−pLSG3T7 mixtures.

*Intracellular Gene Targeting by PNA−Psoralen Conjugates.* A total of 1 × 10$^6$ cells were plated in 100-mm plates 24 h prior to transfection. Cells were transfected with pLSG3T7 using GenePorter 2 (Gene Therapy Systems, Inc.) at 2 $\mu$g of plasmid/10$^6$ cells. After 24 h, PNA2462 was transfected at a 5 $\mu$M concentration via electroporation (Bio-Rad, setting 25 $\mu$F/250 W/250 V, using 0.4-cm cuvette) into cells. UVA irradiation was given (or not) 16 h later at a dose of 1.8 J/cm$^2$ on 100-mm dishes. After UVA irradiation, plasmid DNA was extracted after 48 h and used to transform indicator bacteria for mutant colony selection using the blue−white screen described above. The mutation frequency was calculated and compared, and the mutation pattern was analyzed using DNA-sequencing analysis. A parallel experiment was performed with nonirradiated PNA-transfected cells and compared with the irradiated PNA-transfected cells.

## RESULTS

*Design of PNA Molecules.* It was previously reported that TFOs tethered to psoralen could be used to introduce DNA damage at a targeted region near a TFO-binding site and that this psoralen damage induces mutations and recombination (*33*−*37*). In this study, we examined the feasibility of using bis-PNAs as a tool for site-specific introduction of psoralen adducts for the purpose of targeted gene knockout. A bis-PNA conjugated with psoralen (PNA2462) was designed to form a triplex-invasion complex on the pLSG3T7 plasmid containing a 9-bp polypurine/polypyrimidine target site suitable for triplex-invasion-complex formation and a 5′-TpA base step for photoadduct formation. The bis-PNAs were designed to contain two domains for target-site binding: a Watson−Crick domain to base pair with the polypurine strand on the target duplex and a linked (via ethyleneglycol-type linker) Hoogsteen binding domain designed to bind to the PNA/DNA duplex to form a triple helix (Figure 1A). The substitution of cytosine on the Hoogsteen strand of the PNA with pseudoisocytosine (denoted as J) was used to eliminate the requirement for N3 protonation on cytosines for third-strand binding, which otherwise limits triplex formation to low pH conditions. Three lysines were attached at one end to increase the solubility of the molecules and to enhance the binding affinity to DNA. These modifications serve to increase the rate of strand invasion and to help overcome the pH dependence of Hoogsteen binding (*14*−*16*). Additionally, the bis-PNAs were conjugated with a psoralen derivative, 8-methoxypsoralen, via a connection of the flexible linker (8-amino-2,6-dioxaoctanoic acid) to direct psoralen photoadduct formation at a 5′-TpA, which was 4 bp away from the PNA-binding site. Unlike DNA triplex formation, in which the targeted duplex DNA remains intact and the third strand binds in the major groove, the PNA triplex-invasion complex is composed of an internal $PNA_2$−DNA triplex and a single-stranded DNA loop (p loop). As a result, the duplex/triplex transition in PNA triplex is different from that in DNA triplex. Hence, we designed the PNAs to direct the conjugated psoralen to a 5′-TpA site that is further away from the bis-PNA-strand-invasion complex (4 bp) than we would in the case of TFO binding to an intact duplex in the major groove (1 bp).

*Site-Specific Photoadduct Formation by bis-PNAs Conjugated with Psoralen.* As a prelude to assessing PNA-directed photoadduct formation, we measured PNA binding to the target plasmid using a gel-mobility shift assay. After incubation of increasing concentrations of PNA2462 with plasmid pLSG3T7, the plasmid DNA was digested with restriction enzymes to generate a 158-bp fragment containing the PNA target site, and the products were visualized by gel electrophoresis under native conditions (Figure 1C). To assay the ability of bis-PNAs conjugated with psoralen to introduce site-specific photoadduct formation, we set up a transcription elongation arrest assay using T7 phage RNA polymerase. Plasmid pLSG3T7 contains the T7 promoter downstream of the *supFLSG3* coding region so that *in vitro* transcription using T7 RNA polymerase will use the top strand as a template, as depicted in Figure 1B. In this case, in the absence of photoadduct formation, there is no inhibitory effect of the PNAs on the elongation of RNA polymerase because the triplex-invasion complex is formed on the purine strand of the duplex (lower strand), which is the non-template strand for the T7 RNA polymerase. If there is psoralen photoadduct formation directed by the PNAs on the template strand after UVA irradiation, the adduct on the template strand should block polymerase progression, yielding a

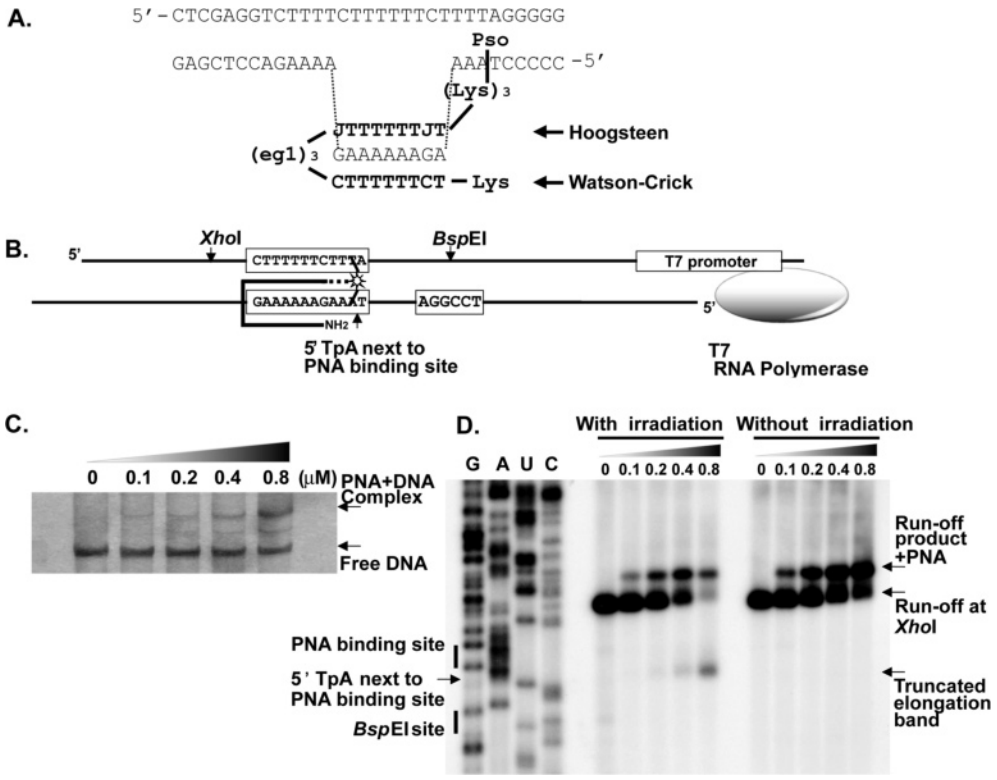


FIGURE 1: Analysis of photoadducts formed by bis-PNAs conjugated with psoralen. (A) PNA binding and triplex-invasion-complex formation on the polypurine strand on the *supFLSG3* gene from position 88 to 96. The bis-PNAs, in which two PNA strands (one strand for Watson−Crick base pairing and the other strand for Hoogsteen base pairing) are chemically linked via a flexible linker, bind to the target site by the strand-invasion process to form a triplex-invasion complex, containing a PNA/DNA/PNA triplex strand and a displaced DNA strand. In addition, the substitution of all cytosines in the Hoogsteen strand with the pseudoisocytosine J monomer (a nucleobase analogue of N3-protonated cytosine) can improve the PNA binding at neutral pH. In PNA2462, psoralen is attached at the N-terminal end via two flexible linkers. (B) Target site for PNA2462 on pLSG3T7. The target site is composed of two domains: 9-bp GA-rich sequences for PNA binding and a 5′-TpA site for photoadduct formation by psoralen. The psoralen intercalation site is 3-bp away from the PNA-binding site. There are two restriction enzyme sites, *Xho*I and *Bsp*EI, around the PNA-binding site, and there is a T7 promoter downstream of the target. This promoter was used in the transcription elongation arrest assay using T7 RNA polymerase. (C) Analysis of PNA2462 binding to pLSG3T7 by gel-shift assay. Various concentrations of PNAs were incubated with a desired amount of pLSG3T7 in TE buffer (pH 7.4) in the presence of 10 mM KCl at 37 °C for 2 h. PNA−pLSG3T7 mixtures were digested by restriction enzymes (*Xho*I/*Bam*HI) to generate a 158-bp fragment and analyzed in 8% polyacrylamide gel in TBE buffer in the absence of photoadduct formation. DNA bands were visualized by silver staining. (D) Determination of photoadduct formation sites by transcription elongation arrest assay using T7 RNA polymerase. After triplex-invasion-complex formation, PNA2462−pLSG3T7 mixtures were UVA-irradiated (or not) at a dose of 1.8 J/cm$^2$ on ice. Transcription elongation arrest assays were performed with irradiated or nonirradiated PNA−pLSG3T7 mixtures and analyzed in a 10% denaturing polyacrylamide gel containing 7 M urea in TBE buffer. The site of polymerase arrest was determined by a comparison with the RNA-sequencing ladder. The "run-off product + PNA" band comprises complexes formed by binding of PNAs (which are in large excess) to the synthesized RNA strands containing the homopurine PNA target sequence.

truncated band. PNA2462−pLSG3T7 mixtures containing increasing concentrations of PNA, as indicated, were either irradiated or not, and the polymerase arrest assay was performed (Figure 1D). Polymerase arrest, as visualized by the indicated band corresponding to the transcription product, was only seen in samples receiving UVA irradiation, demonstrating a requirement for photoadduct formation. In addition, the band intensity is also seen to increase with the PNA concentration, showing a PNA dose dependence. When the sequencing ladder shown in the panel was compared, the truncated band position was determined to be the expected psoralen intercalation site at the 5′-TpA dinucleotide, next to the PNA-binding site (Figure 1D). These results demonstrate that bis-PNAs conjugated to psoralen can introduce site-specific photoadducts on the target duplex DNA.

*PNA Concentration and UV Irradiation Dose-Dependent Kinetics of Photoadduct Formation.* Using the same T7 polymerase arrest assay as in Figure 1, we examined in detail the dependence of PNA binding and targeted photoadduct formation on the PNA concentration (parts A and B of Figure 2). This experiment also allowed a correlation of the extent of PNA binding with the efficiency of photoadduct formation (Figure 2C). Photoadduct formation efficiency was derived from the ratio between the run-off product and the truncated elongation band. We compared the photoadduct formation efficiency with the binding efficiency of PNAs and presented the two efficiencies as a function of the PNA concentration. At the highest concentration of PNA tested (0.8 $\mu$M), 74% of the target plasmid was bound by the PNAs with 50% of plasmid having photoadducts.

UVA dose dependence of targeted photoadduct formation was also measured by the transcription elongation arrest assay, with PNA−pLSG3T7 mixtures irradiated over a range of doses from 0 to 3.6 J/cm$^2$, corresponding to irradiation times of 0−12 min (parts D and E of Figure 2). In Figure 2D, as the irradiation dose increased, there was an increasing amount of photoadduct formation, as visualized by the truncated elongation bands. Photoadduct formation efficiency was derived and is presented as a function of the UVA

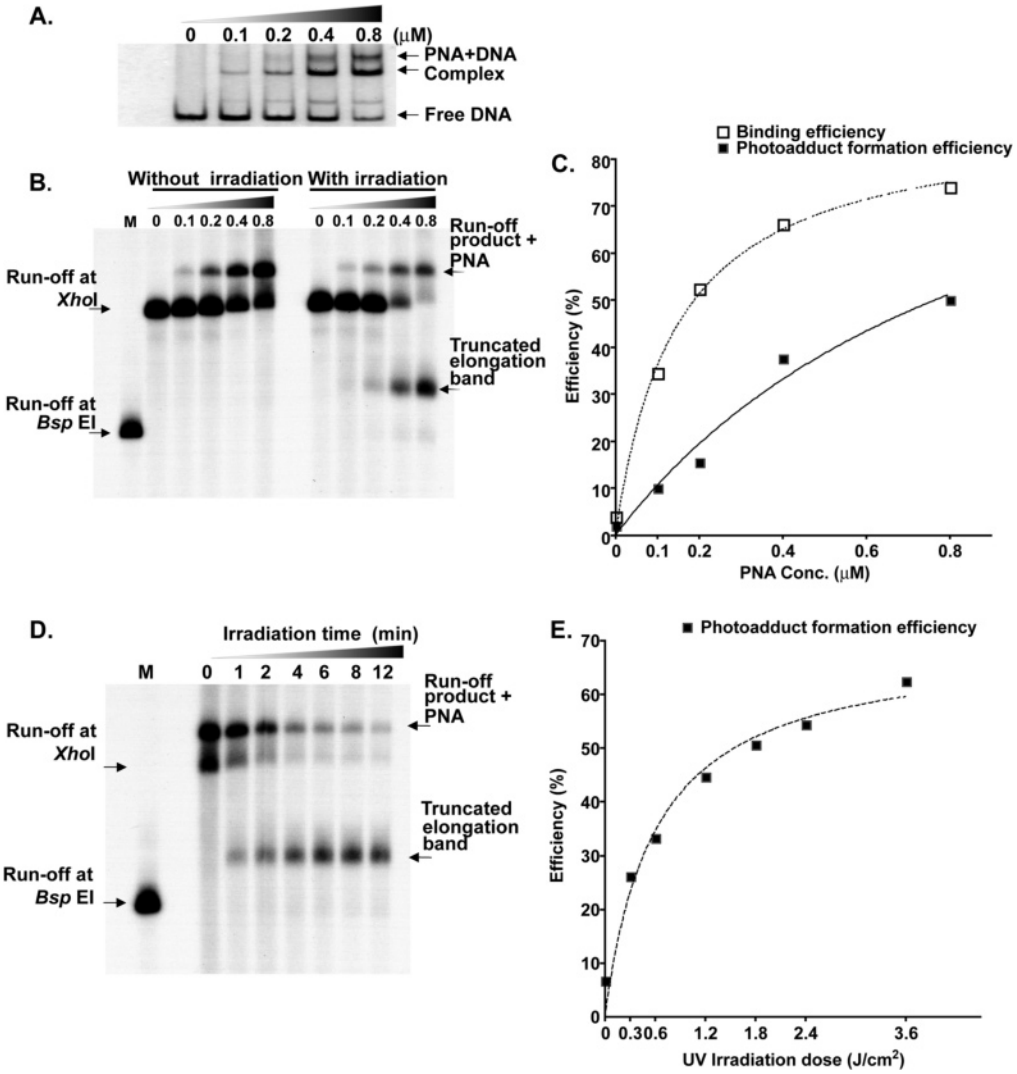


FIGURE 2: Concentration and UVA dose dependence of photoadduct formation. (A) Binding efficiency of PNA2462 to pLSG3T7 analyzed by gel-shift assay. After triplex-invasion-complex formation with various concentrations of PNA2462 (as indicated), PNA−pLSG3T7 mixtures were digested with restriction enzymes (*Xho*I/*Bam*HI) and analyzed in 8% polyacrylamide gels in TBE. DNA bands were visualized by silver staining. The binding efficiency was derived from the ratio between PNA-bound and nonbound DNA fragments. The PNA−DNA complexes involved in the major band represent the PNA clamp bound on the DNA target in a 1:1 ratio. The minor band of slower mobility likely represents 2PNA−1DNA complexes that form at high PNA concentrations (*47*). (B) Concentration dependence of photoadduct formation. The autoradiogram shows the concentration dependence of photoadduct formation. Transcription elongation arrest assays were performed with irradiated or nonirradiated PNA−pLSG3T7 mixtures described in B and analyzed in 10% denaturing polyacrylamide gel containing 7 M urea in TBE buffer. As an RNA size marker, the run-off product of *Bsp*EI-linearized pLSG3T7 was included. The photoadduct formation efficiency was derived from the ratio between the run-off product and the truncated elongation band. (C) Comparison of the binding and the photoadduct formation efficiencies. The binding and the photoadduct formation efficiencies were fitted by Prism (GraphPad Software, Inc.) and were presented with the binding efficiency of PNAs, as a function of the PNA concentration. (D) Irradiation dose dependence of photoadduct formation. The autoradiogram shows UVA dose dependence of photoadduct formation. After triplex-invasion-complex formation at a 0.8 $\mu$M PNA concentration, transcription elongation arrest assays were performed with PNA−pLSG3T7 mixtures, which were UVA-irradiated for 0−12 min, representing the indicated UVA doses. Transcription products were analyzed as described in C. (E) Photoadduct formation efficiency. The photoadduct formation efficiency was fitted by Prism (GraphPad Software, Inc.) and was presented as a function of the UVA dose. The photoadduct formation efficiency was determined in a single assay; thus, no error bars are shown.

irradiation time (Figure 2E). There was 51% photoadduct formation efficiency with 1.8 J/cm$^2$ of UVA irradiation (under conditions of 74% PNA-binding efficiency with 0.8 $\mu$M PNA), which would yield a photomodification efficiency of approximately 66%. When the above results are taken together, they demonstrate that bis-PNAs conjugated with psoralen can introduce site-specific photoadducts at a specific base pair in the target DNA in a concentration- and UVA-irradiation-dependent manner.

*Mutagenic Effects of bis-PNA Conjugated with Psoralen in Cells Measured by Shuttle Vector Assay.* To test the ability of bis-PNA conjugated with psoralen to induce site-specific mutations in DNA, an episomal shuttle vector assay was performed in mammalian cells. The method used to examine the targeted mutagenesis is illustrated in Figure 3A. In this analysis, the SV40-based shuttle vector pLSG3T7 was used, as in previous work with TFOs conjugated with psoralen (*32*). This vector contains the *supFLSG3* mutation-reporter gene, which encodes an amber suppressor tRNA. At the 5′ end of the gene, there is a PNA-binding domain consisting of a 9-bp A:T-rich sequence from positions 88 to 96 upstream of the coding region. Next to the PNA-binding site, there is a 5′-TpA base step for psoralen intercalation and photoadduct formation at positions 99−100, just at the start of the coding

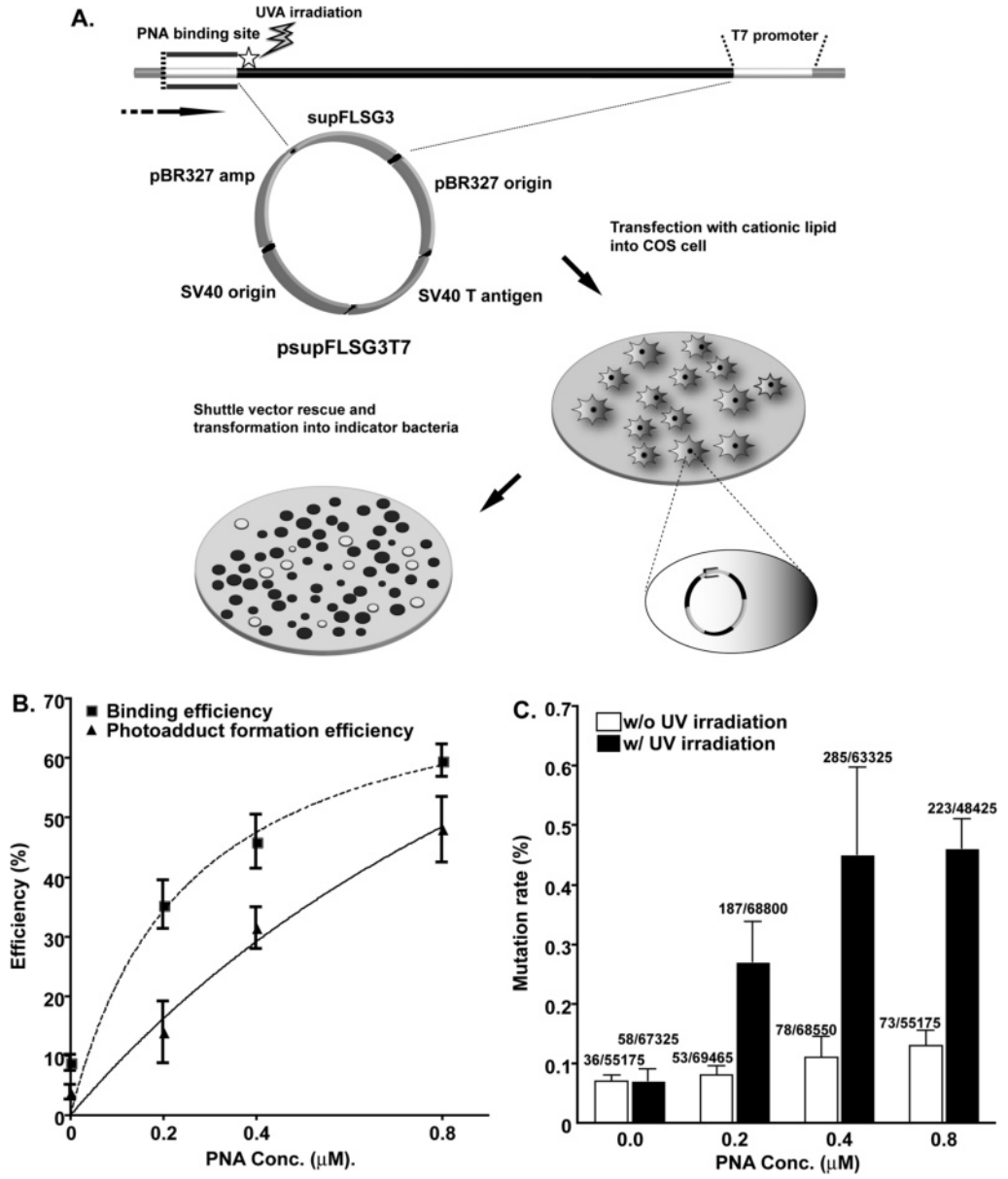


FIGURE 3: Targeted mutagenesis by bis-PNAs conjugated with psoralen in mammalian cells. (A) Experimental scheme of the shuttle vector rescue assay to measure the mutagenic effect of bis-PNAs conjugated to psoralen. After triplex-invasion-complex formation with PNA2462 and pLSG3T7, PNA2462−pLSG3T7 mixtures were UVA-irradiated (or not) at a dose of 1.8 J/cm$^2$ for photoadduct formation. UVA irradiated (or not) PNA−pLSG3T7 mixtures were transfected via cationic lipids into COS cells. After 48 h, plasmid DNA was extracted for shuttle vector rescue assay and retransformed into indicator bacteria for DNA analysis of the *supFLSG3* gene. (B) Comparison of binding and photoadduct formation efficiencies. After triplex-invasion-complex formation and UVA irradiation, the binding and photoadduct formation efficiencies of PNA2462 were determined as described. These efficiencies were fitted and presented as a function of the PNA concentration. Error bars indicate standard error. (C) Mutation rates induced by bis-PNAs conjugated with psoralen. Mutation rates of UVA-irradiated or nonirradiated psoralen-bis-PNA/vector complexes transfected into COS cells were derived from the frequency of white colonies (representing mutants) out of the total colonies and presented as a function of the PNA concentration. Error bars indicate standard error.

region of the *supFLSG3* gene. Point mutations within the PNA-binding site are not detectable because such mutations do not inactivate the function of the *supFLSG3* gene. However, deletion mutations extending into the coding region of the *supFLSG3* gene near the PNA-binding site or point mutations at the 5′-TpA dinucleotide are detectable.

Triplex-invasion complexes were preformed prior to transfection into COS cells by co-incubation of the PNA and pLSG3T7 in TE (pH 7.4) at 37 °C for 2 h, followed by UVA irradiation to form photoadducts. The UVA-irradiated PNA−pLSG3T7 mixtures were transfected into COS cells via cationic lipids, and, 48 h later, the episomal pLSG3T7 DNA was isolated for the analysis of mutagenesis in the *supFLSG3* gene via transfection into indicator bacteria. The mutation frequency was determined and presented as a function of the PNA concentration (Figure 3C). In each experiment, the binding efficiency and photoadduct-formation efficiency was determined and compared with the mutation frequency. A parallel experiment with nonirradiated PNA−pLSG3T7 samples was performed for a comparison (parts B and C of Figure 3). With the irradiated PNA−pLSG3T7 mixtures, there was a PNA dose-dependent induction of mutations. At a concentration of 0.8 $\mu$M, there was a 47.9% photoadduct yield and an induced mutation frequency of 0.46%, 6.5-fold above the background. With the nonirradiated PNA−pLSG3T7 mixture at the 0.8 $\mu$M PNA concentration, the

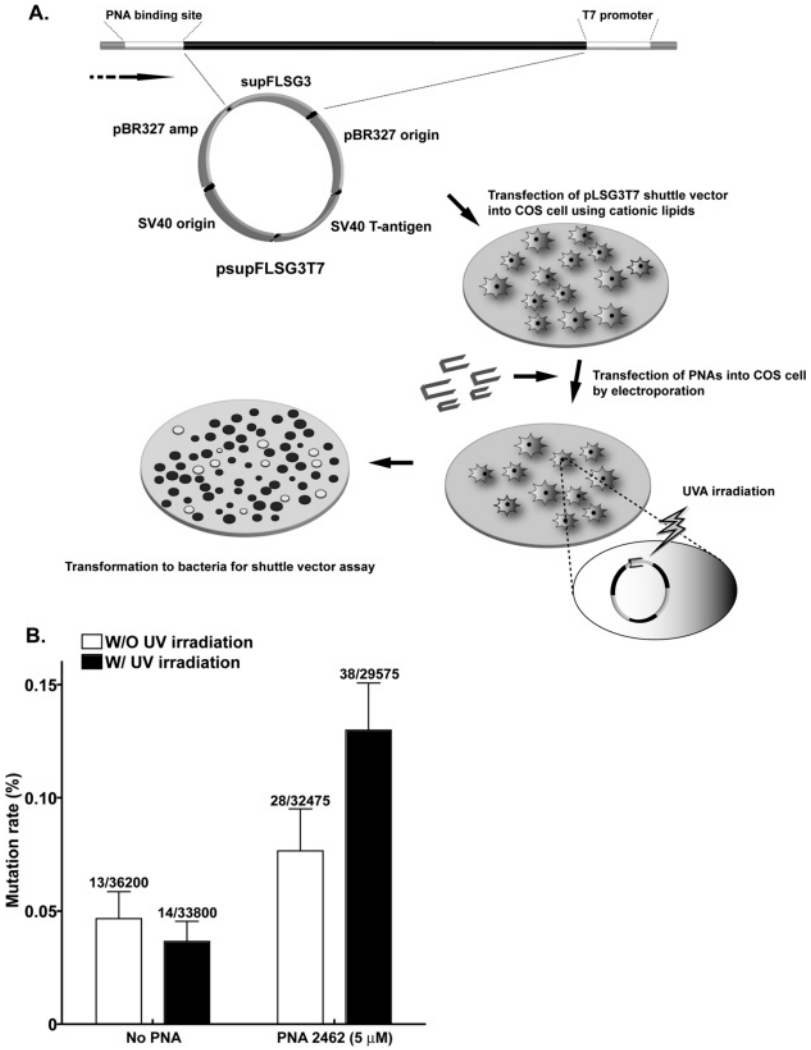


FIGURE 4: Intracellular gene targeting by bis-PNAs conjugated with psoralen. (A) Experimental scheme for assaying intracellular gene targeting. The cells were pretransfected with pLSG3T7 vector via cationic lipids, followed by transfection of PNAs, at a concentration of 5 $\mu$M, using electroporation. After 16 h for intracellular triplex-invasion-complex formation, the cells were UVA irradiated (or not) for photoadduct formation by psoralen. DNA was extracted after 48 h and used to transform indicator bacteria to assay supF gene function frequencies. (B) Mutation frequencies induced by intracellular gene targeting by PNAs. Induced mutation frequencies by PNAs were determined as described and compared. Error bars indicate standard error.

induced mutation frequency was 0.13%, 1.9-fold higher than the background. These results indicate that bis-PNAs bound to duplex DNA via the triplex-strand-invasion complex can mediate site-specific introduction of psoralen photoadducts on the target DNA, yielding gene-targeted mutations in mammalian cells.

*Intracellular Gene Targeting by PNAs Conjugated to Psoralen.* The intracellular gene-targeting ability of PNAs linked to psoralen was examined using the pLSG3T7 shuttle vector in an intracellular targeting assay, as in our previous work with TFOs conjugated with psoralen. The protocol used to investigate intracellular targeting is illustrated in Figure 4A. COS cells were pretransfected with pLSG3T7 on day 1 to establish the episomal target in the cells, followed on day 2 by transfection via electroporation with the psoralen−bis-PNA. After 16 h, to allow for intracellular uptake and for triplex-invasion-complex formation by the PNAs, cells were UVA-irradiated (or not) at a dose of 1.8 J/cm$^2$ for psoralen photoactivation. The plasmid DNA was extracted 48 h later and used to transform indicator bacteria for analysis of mutagenesis in the *supFLSG3* gene. Mutation frequencies were determined as above (Figure 4B). In the absence of UVA irradiation, the PNA yielded a mutation frequency of 0.08%, 2-fold above the background. With UVA irradiation, the induced mutation frequency was 0.13%, 3.5-fold higher than the background. These results indicate that PNAs can mediate intracellular gene targeting and deliver conjugated DNA-reactive agents.

*Analysis of Mutations Induced by Psoralen-Conjugated PNAs.* The pattern of mutations induced by bis-PNAs conjugated to psoralen was analyzed by sequence analysis of 79 independent mutant colonies (Figure 5). These mutations were compiled from the transfection of UVA-irradiated pso-bis-PNA−pLSG3T7 mixtures into COS cells. The majority of the mutations contained deletions around the PNA-binding and photoadduct-formation sites (bp 86−100). Interestingly, many deletions occurred between regions of microhomology of either 4 or 6 bp (underlined). Such a pattern is consistent with the generation of double-strand breaks that are repaired by end-joining reactions (*38*). [A similar pattern of deletions with joints at regions of microhomology was found in a study of mutagenesis mediated by psoralen-conjugated TFOs (*36*, *39*, *40*).] In addition, point mutations consisting of base-pair substitutions and single-

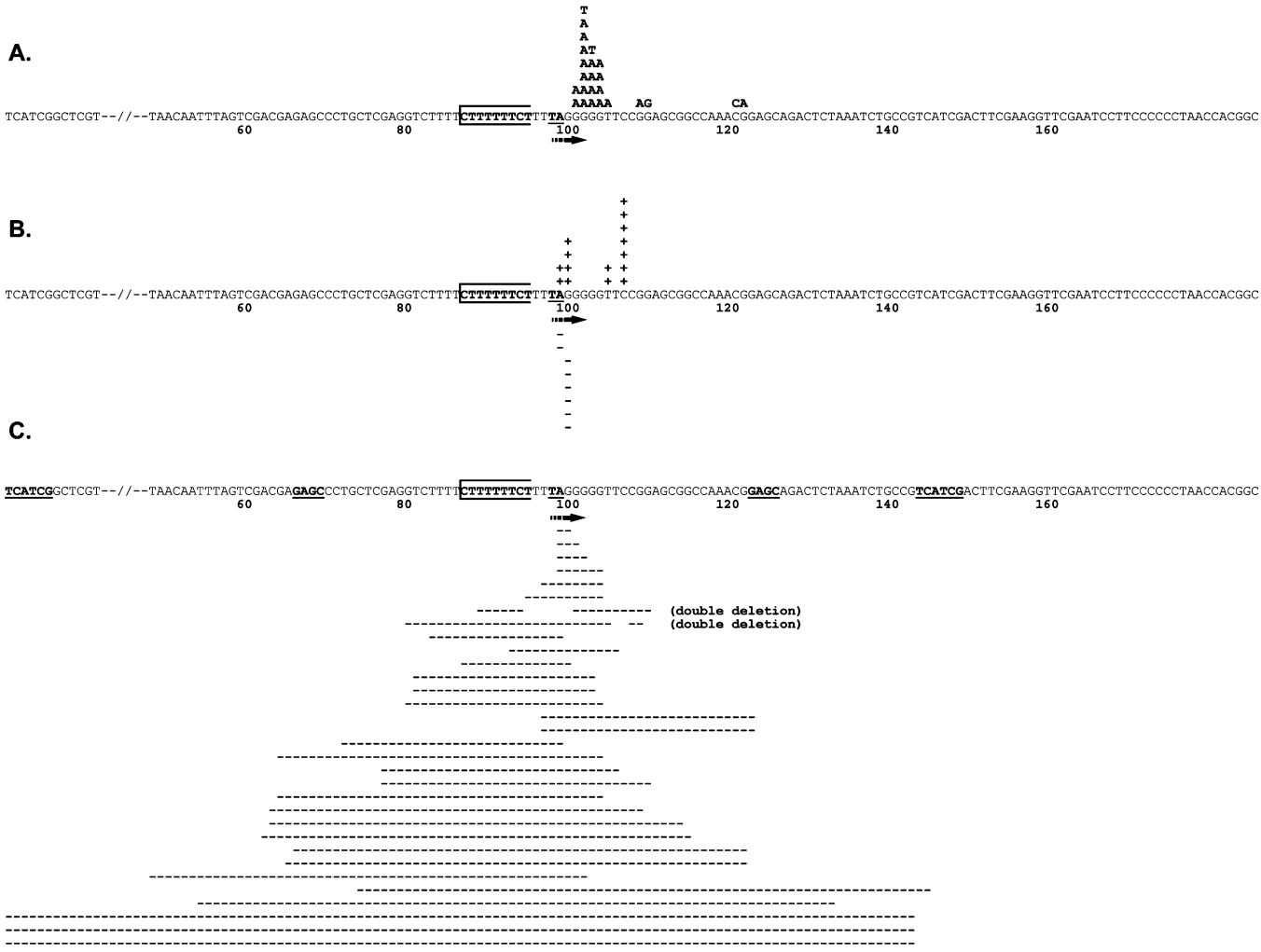


FIGURE 5: Mutation patterns in the *supFLSG3* gene induced by bis-PNAs conjugated with psoralen. Mutation patterns induced by PNA2462 plus UVA irradiation were analyzed by sequence analysis. The PNA-binding site is indicated by the lines above and below the gene sequence at base pairs 88−96. The start region of the *supFLSG3* gene (position 99) is indicated by an arrow. (A) Base substitutions. The single-base substitutions are listed above the corresponding *supFLSG3* gene sequence. (B) Single-base-pair insertions or deletions. The single-base-pair insertions are indicated by "+" above the mutated site, and deletions are indicated by "−" below the mutation site. In all cases, mutations shown consisted of single-point mutations. (C) Deletions greater than one base pair. A dashed line below the gene sequence indicates the extent of the deletion for each mutant. One mutant is shown per line. In two cases, noncontiguous segments were deleted in a single mutant, as indicated. Frequent deletion joint regions containing 4−6 bp of microhomology are underlined in the sequence.

base-pair insertions and deletions were found at or adjacent to the psoralen intercalation site. When these results are taken together, they demonstrate that bis-PNAs conjugated to psoralen can mediate the introduction of site-specific photoadducts and mutations in target duplex DNAs.

## DISCUSSION

The overall purpose of this study was to explore the feasibility of using PNAs conjugated to psoralen as site-specific gene modification tools. Our previous studies on site-specific gene modification with TFOs conjugated with psoralen demonstrated that the binding characteristics and sequence specificity of TFOs could be used to direct linked DNA-reactive molecules to produce targeted DNA damage and mutations (*32*−*34*, *37*). In this study, we tested psoralen-linked bis-PNAs instead of TFOs, on the basis of the ability of bis-PNAs to make very stable triplex-invasion complexes at relatively short polypurine runs (*6*). TFOs may also be useful as gene-targeting reagents for applications *in vivo*, but there are some limitations to the activity of TFOs and triplex stability. Triplexes formed by pyrimidine TFOs are sensitive to physiological pH because of the need for cytosine protonation requiring of the use of C analogues (41). The activity of G-rich TFOs is compromised by physiological levels of $K^+$, which favor the formation of G quartets (42). Both motifs also require divalent metal cations, particularly $Mg^{2+}$, for high affinity. One advantage of using PNAs instead of TFOs is the potentially higher stability of bis-PNAs once bound to the target sequence. However, the rate of strand invasion by bis-PNAs is inhibited by high salt concentrations in cells, although cellular processes such as transcription and replication may transiently open the duplex and enhance the capacity of the bis-PNAs to strand invade (*24*, *43*). In addition, various modifications of PNAs, such as the addition of lysine residues at one end or the use of modified nucleobases, can increase the rate of strand invasion under physiological conditions (*15*, *16*). Also, the pseudopeptide backbone of PNAs is resistant to both protease and nuclease activity *in vivo*; thus, PNAs are relatively stable molecules (*44*). These features make the design and application of PNAs potentially advantageous.

To examine the ability of psoralen−bis-PNAs to mediate targeted mutagenesis, we designed the bis-PNA conjugated with psoralen to generate site-specific photoadducts within the *supFLSG3* gene. Our results show that such PNAs can mediate photoadduct formation at the predicted 5′-TpA site, next to the PNA-binding site. The photoadduct formation showed a PNA concentration and UVA dose dependence. The shuttle vector mutagenesis assay showed that bis-PNA-targeted photoadducts could induce mutations in a site-specific manner. With *in vitro* PNA binding and photoadduct formation, mutation frequencies of up to 0.46% were produced, 6.5-fold higher than the background. In the assay for intracellular gene targeting, which requires both PNA binding and photoadduct formation to occur in the episomal target within cells, mutation frequencies in the range of 0.13% were seen, 3.5-fold higher than the background. Because the type of episomal SV40-based shuttle vector used in our studies has been previously shown to be chromatinized (*45*), the results provide some encouragement that endogenous chromosomal DNA may also be targeted for adduct formation by pso-PNAs.

All of the point mutations that we could detect were found to occur at or downstream of the targeted psoralen adduct site at base pairs 99−100. It is theoretically possible that other point mutations were also produced by the PNAs at base pairs upstream of position 99 (*26*). However, the region upstream of position 99 is not within the *supF* coding region; thus, mutation in this region is not detectable. Because a number of point mutations are, therefore, potentially missed in the assay, the induced mutation frequencies presented in Figures 3 and 4 are likely underestimates of the actual efficiencies of psoralen−PNA-induced mutagenesis.

Interestingly, most of the deletions in this study appear to have occurred between sites containing 4−6 bp of homology, suggesting an end-joining process (*38*). It is likely that the deletions were produced by psoralen−PNA-induced double-strand breaks, which are then repaired by end joining at regions of microhomology following exonuclease activity. This pattern of deletions is consistent with that produced by psoralen−TFOs in a previous study (*36*, *39*, *40*), suggesting that a similar mechanism may resolve both bis-PNA and TFO-targeted psoralen cross-links.

Progress has been made within the past few years toward the development of PNAs as DNA-binding molecules for site-specific gene modification and regulation. The results presented here demonstrate the feasibility of using PNAs conjugated to psoralen to introduce site-specific photoadducts, and they show the biological effect of such photoadducts in mammalian cells. The frequency of intracellular targeting by the pso-PNAs at 0.13% will likely need to be increased for practical application to most disease-related genes. However, in some cases, a low frequency may be sufficient if there is a relative advantage conferred on cells in which a targeting event has occurred, such as would be the case with targeted knock-out of the CCR5 gene that encodes the HIV coreceptor. Nonetheless, PNA technology still has several problems to be solved, such as a cellular uptake and the sequence restriction for Hoogsteen base paring for clamp formation. To this end, various methods are being developed to enhance delivery of PNAs into mammalian cells, such as conjugation of PNAs to cationic peptides that mediate cellular uptake (*25*, *46*). In addition, the development of pseudocomplementary PNAs, which can bind duplex DNA at nonpolypurine regions via Watson−Crick double-strand invasion complexes (*21*), may help to overcome the sequence restriction of bis-PNA technology.

## REFERENCES


1. Kuan, J. Y., and Glazer, P. M. (2004) Targeted gene modification using triplex-forming oligonucleotides, *Methods Mol. Biol. 262*, 173−194.
2. Nielsen, P. E. (2004) PNA technology, *Mol. Biotechnol. 26*, 233−248.
3. White, S., Szewczyk, J., Turner, J., Barid, E., and Dervan, P. (1998) Recognition of the four Watson−Crick base pairs in the DNA minor groove by the synthetic ligands, *Nature 391*, 468−471.
4. Klug, A. (1999) Zinc finger peptides for the regulation of gene expression, *J. Mol. Biol. 293*, 215−218.
5. Nielsen, P., Egholm, M., Berg, R., and Buchardt, O. (1991) Sequence-selective recognition of DNA by strand displacement with a thymine-substituted polyamide, *Science 254*, 1497−1500.
6. Egholm, M., Buchardt, O., Christensen, L., Behrens, C., Freier, S., Driver, D., Berg, R., Kim, S., Norden, B., and Nielsen, P. (1993) PNA hybridizes to complementary oligonucleotides obeying the Watson−Crick hydrogen-bonding rules, *Nature 365*, 566−568.
7. Jensen, K., Orum, H., Nielsen, P., and Norden, B. (1997) Kinetics for Hybridization of peptide nucleic acids (PNA) with DNA and RNA studied with the BIAcore technique, *Biochemistry 36*, 5072−5077.
8. Wittung, P., Nielsen, P. E., Buchardt, O., Egholm, M., and Norden, B. (1994) DNA-like double helix formed by peptide nucleic acid, *Nature 368*, 561−563.
9. Nielsen, P. E., Egholm, M., and Buchardt, O. (1994) Evidence for (PNA)2/DNA triplex structure upon binding of PNA to dsDNA by strand displacement, *J. Mol. Recognit. 7*, 165−170.
10. Cherny, D., Belotserkovskii, B., Frank-Kamenetskii, M., Egholm, M., Buchardt, O., Berg, R., and Nielsen, P. (1993) DNA unwinding upon strand-displacement binding of a thymine-substituted polyamide to double-stranded DNA, *Proc. Natl. Acad. Sci. U.S.A. 90*, 1667−1670.
11. Nielsen, P., and Christensen, L. (1996) Strand displacement binding of a duplex-forming homopurine PNA to a homopyrimidine duplex DNA target, *J. Am. Chem. Soc. 118*, 2287−2288.
12. Kurakin, A., Larsen, H. J., and Nielsen, P. E. (1998) Cooperative strand displacement by peptide nucleic acid (PNA), *Chem. Biol. 5*, 81−89.
13. Peffer, N. J., Hanvey, J. C., Bisi, J. E., Thomson, S. A., Hassman, C. F., Noble, S. A., and Babiss, L. E. (1993) Strand-invasion of duplex DNA by peptide nucleic acid oligomers, *Proc. Natl. Acad. Sci. U.S.A. 90*, 10648−10652.
14. Kuhn, H., Demidov, V., Frank-Kamenetskii, M., and Nielsen, P. (1998) Kinetic sequence discrimination of cationic bis-PNAs upon targeting of double-stranded DNA, *Nucleic Acids Res. 26*, 582−587.
15. Griffith, M., Risen, L., Greig, M., Lesnik, E., Sprankle, K., Griffey, R., Kiely, J., and Freier, S. (1995) Single and bis peptide nucleic acids as triplexing agents: Binding and stoichiometry, *J. Am. Chem. Soc. 117*, 831−832.
16. Egholm, M., Christensen, L., Dueholm, L., Buchardt, O., Coull, J., and Nielsen, P. (1995) Efficient pH-independent sequence-specific DNA binding by pseudoisocytosine-containing bis-PNA, *Nucleic Acids Res. 23*, 217−222.
17. Hanvey, J. C., Peffer, N. J., Bisi, J. E., Thomson, S. A., Cadilla, R., Josey, J. A., Ricca, D. J., Hassman, C. F., Bonham, M. A., Au, K. G., et al. (1992) Antisense and antigene properties of peptide nucleic acids, *Science 258*, 1481−1485.
18. Nielsen, P. E., Egholm, M., and Buchardt, O. (1994) Sequence-specific transcription arrest by peptide nucleic acid bound to the DNA template strand, *Gene 149*, 139−145.
19. Vickers, T. A., Griffith, M. C., Ramasamy, K., Risen, L. M., and Freier, S. M. (1995) Inhibition of NF-$\kappa$ B specific transcriptional activation by PNA strand invasion, *Nucleic Acids Res. 23*, 3003−3008.
20. Praseuth, D., Grigoriev, M., Guieysse, A. L., Pritchard, L. L., Harel-Bellan, A., Nielsen, P. E., and Helene, C. (1996) Peptide

nucleic acids directed to the promoter of the α-chain of the interleukin-2 receptor, *Biochim. Biophys. Acta. 1309*, 226−238.
21. Lohse, J., Dahl, O., and Nielsen, P. E. (1999) Double duplex invasion by peptide nucleic acid: A general principle for sequence-specific targeting of double-stranded DNA, *Proc. Natl. Acad. Sci. U.S.A. 96*, 11804−11808.
22. Mollegaard, N. E., Buchardt, O., Egholm, M., and Nielsen, P. E. (1994) Peptide nucleic acid−DNA strand displacement loops as artificial transcription promoters, *Proc. Natl. Acad. Sci. U.S.A. 91*, 3892−3895.
23. Wang, G., Xu, X., Pace, B., Dean, D. A., Glazer, P. M., Chan, P., Goodman, S. R., and Shokolenko, I. (1999) Peptide nucleic acid (PNA) binding-mediated induction of human γ-globin gene expression, *Nucleic Acids Res. 27*, 2806−2813.
24. Diviacco, S., Rapozzi, V., Xodo, L., Helene, C., Quadrifoglio, F., and Giovannangeli, C. (2001) Site-directed inhibition of DNA replication by triple helix formation, *FASEB J. 15*, 2660−2668.
25. Rogers, F. A., Manoharan, M., Rabinovitch, P., Ward, D. C., and Glazer, P. M. (2004) Peptide conjugates for chromosomal gene targeting by triplex-forming oligonucleotides, *Nucleic Acids Res. 32*, 6595−6604.
26. Faruqi, A. F., Egholm, M., and Glazer, P. M. (1998) Peptide nucleic acid-targeted mutagenesis of a chromosomal gene in mouse cells, *Proc. Natl. Acad. Sci. U.S.A. 95*, 1398−1403.
27. Rogers, F. A., Vasquez, K. M., Egholm, M., and Glazer, P. M. (2002) Site-directed recombination via bifunctional PNA−DNA conjugates, *Proc. Natl. Acad. Sci. U.S.A. 99*, 16695−16700.
28. Armitage, B., Koch, T., Frydenlund, H., Orum, H., Batz, H. G., and Schuster, G. B. (1997) Peptide nucleic acid−anthraquinone conjugates: Strand invasion and photoinduced cleavage of duplex DNA, *Nucleic Acids Res. 25*, 4674−4678.
29. Ross, G. F., Smith, P. M., McGregor, A., Turnbull, D. M., and Lightowlers, R. N. (2003) Synthesis of trifunctional PNA-benzophenone derivatives for mitochondrial targeting, selective DNA binding, and photo-cross-linking, *Bioconjugate Chem. 14*, 962−966.
30. Okamoto, A., Tanabe, K., and Saito, I. (2001) Synthesis and properties of peptide nucleic acids containing a psoralen unit, *Org. Lett. 3*, 925−927.
31. Cimino, G., Shi, Y., and Hearst, J. (1985) Psoralens as photoactive probes of nucleic acid structure and function: Organic chemistry, photochemistry, and biochemistry, *Annu. Rev. Biochem. 54*, 1151−1193.
32. Lacroix, L., Lacoste, J., Reddoch, J. F., Mergny, J. L., Levy, D. D., Seidman, M. M., Matteucci, M. D., and Glazer, P. M. (1999) Triplex formation by oligonucleotides containing 5-(1-propynyl)-2′-deoxyuridine: Decreased magnesium dependence and improved intracellular gene targeting, *Biochemistry 38*, 1893−1901.
33. Wang, G., Levy, D. D., Seidman, M. M., and Glazer, P. M. (1995) Targeted mutagenesis in mammalian cells mediated by intracellular triple helix formation, *Mol. Cell. Biol. 15*, 1759−1768.
34. Vasquez, K. M., Dagle, J. M., Weeks, D. L., and Glazer, P. M. (2001) Chromosome targeting at short polypurine sites by cationic triplex-forming oligonucleotides, *J. Biol. Chem. 276*, 38536−38541.
35. Luo, Z., Macris, M. A., Faruqi, A. F., and Glazer, P. M. (2000) High-frequency intrachromosomal gene conversion induced by triplex-forming oligonucleotides microinjected into mouse cells, *Proc. Natl. Acad. Sci. U.S.A. 97*, 9003−9008.
36. Majumdar, A., Khorlin, A., Dyatkina, N., Lin, F. L., Powell, J., Liu, J., Fei, Z., Khripine, Y., Watanabe, K. A., George, J., Glazer, P. M., and Seidman, M. M. (1998) Targeted gene knockout mediated by triple helix forming oligonucleotides, *Nat. Genet. 20*, 212−214.
37. Havre, P. A., Gunther, E. J., Gasparro, F. P., and Glazer, P. M. (1993) Targeted mutagenesis of DNA using triple helix-forming oligonucleotides linked to psoralen, *Proc. Natl. Acad. Sci. U.S.A. 90*, 7879−7883.
38. Chu, G. (1997) Double strand break repair, *J. Biol. Chem. 272*, 24097−24100.
39. Puri, N., Majumdar, A., Cuenoud, B., Natt, F., Martin, P., Boyd, A., Miller, P. S., and Seidman, M. M. (2001) Targeted gene knockout by 2′-*O*-aminoethyl modified triplex forming oligonucleotides, *J. Biol. Chem. 276*, 28991−28998.
40. Raha, M., Wang, G., Seidman, M. M., and Glazer, P. M. (1996) Mutagenesis by third-strand-directed psoralen adducts in repair-deficient human cells: High frequency and altered spectrum in a Xeroderma pigmentosum variant, *Proc. Natl. Acad. Sci. U.S.A. 93*, 2941−2946.
41. Singleton, S. F., and Dervan, P. B. (1992) Influence of pH on the equilibrium association constants for oligodeoxyribonucleotide-directed triple helix formation at single DNA sites, *Biochemistry 31*, 10995−11003.
42. Williamson, J. R., Raghuraman, M. K., and Cech, T. R. (1989) Monovalent cation-induced structure of telomeric DNA: The G-quartet model, *Cell 59*, 871−880.
43. Larsen, H. J., and Nielsen, P. E. (1996) Transcription-mediated binding of peptide nucleic acid (PNA) to double-stranded DNA: Sequence-specific suicide transcription, *Nucleic Acids Res. 24*, 458−463.
44. Demidov, V., Potaman, V., Frank-Kamenetskii, M., Egholm, M., Buchard, O., Sonnichsen, S., and Nielsen, P. (1994) Stability of peptide nucleic acids in human serum and cellular extracts, *Biochem. Pharmacol. 48*, 1310−1313.
45. Cereghini, S., and Yaniv, M. (1984) Assembly of transfected DNA into chromatin: Structural changes in the origin−promoter−enhancer region upon replication, *EMBO J. 3*, 1243−1253.
46. Kaihatsu, K., Huffman, K. E., and Corey, D. R. (2004) Intracellular uptake and inhibition of gene expression by PNAs and PNA−peptide conjugates, *Biochemistry 43*, 14340−14347.
47. Hansen, G. I., Bentin, T., Larsen, H. J., and Nielsen, P. E. (2001) Structural isomers of bis-PNA bound to a target in duplex DNA, *J. Mol. Biol. 307*, 67−74.

BI051379A